Ultrathin films of Pt on TiO_2(110): Growth and chemisorption-induced surfactant effects

Hans-Peter Steinrück,* François Pesty,† Lei Zhang, and Theodore E. Madey
Department of Physics and Astronomy, Laboratory for Surface Modification, Rutgers, The State University of New Jersey, Piscataway, New Jersey 08855
(Received 10 August 1994)

The growth of ultrathin platinum films on a rutile TiO_2(110) surface has been studied using low-energy ion scattering and x-ray photoelectron spectroscopy. In the temperature range between 160 and 420 K, Pt grows in three-dimensional islands on the TiO_2 surface with the size of the islands increasing with increasing surface temperature and without indication of an interface reaction. Evaporation of Pt in the presence of CO leads to a significantly higher degree of wetting. This behavior is attributed to a chemisorption-induced surfactant effect.

I. INTRODUCTION

The growth of metals on oxide surfaces has received considerable interest recently. In particular the questions of growth mode, interface reactions, and their dependence on surface temperature are of significant interest from a fundamental as well as from an applied point of view. The fundamental interest concerns the understanding of bonding at the metal/oxide interface as well as the kinetics and thermodynamics of the growth process and its dependence on the experimental conditions such as electronic and geometric properties of the substrate, temperature, surface energy, and in particular interfacial energy. The interplay between these energies determines the type of growth mode that is characteristic for a particular system. Applications of metal/oxide interfaces include the further development of new ceramic materials and, very importantly, support materials for heterogeneous catalysis.

The (110) surface of rutile TiO_2 is well suited for such investigations. First of all, the electronic and the geometric properties of this surface are well known; furthermore, it is possible to prepare a stoichiometric TiO_2(110) surface on top of a slightly reduced TiO_2 bulk crystal.[1] The reduced sample is conducting, which significantly simplifies the application of electron spectroscopies. The stoichiometric layer is thin enough that no charging is observed in the experiments.

The growth modes of vapor-deposited thin films are traditionally classified in three main modes.[2] The layer-by-layer mode, called Frank–van der Merwe, represents a two-dimensional growth; the island mode, Volmer-Weber growth, corresponds to the formation of three-dimensional clusters; finally, the intermediate layer-island mode, Stranski-Krastanov growth, is characterized by the formation of one or more monolayers followed by island growth. By considering only energetic arguments, one can see that the growth mode depends on the respective values of surface energies of the substrate and its adsorbate and on the interfacial energy. Of course, the principle of energy minimization is not sufficient to predict growth modes when the deposition does not occur under thermodynamic equilibrium conditions. Then kinetics considerations must be taken into account. It has been claimed, for instance, that an apparent wetting of metals on oxides does not necessarily mean that the metal-oxide adsorption bond is stronger than the metal-metal bond, but rather dynamic effects might intervene when the adsorbing metal atoms are strongly bonded on the oxide surface: in such a case, the diffusion of adatoms at the surface should be hindered and the experimental results on growth could be difficult to interpret unambiguously.[3]

The present study is a continuation of a systematic investigation on the interaction and the growth mode of various metals (Cu, Fe, Cr, and Hf) on the TiO_2(110) surface.[4–7] The initial growth mode of these metals varies from two-dimensional growth of Hf, on the one hand, to three-dimensional growth of Cu, on the other hand.[4] One important conclusion that has been derived is the importance of the reactivity of the TiO_2 surface with respect to a particular metal, i.e., the interfacial energy, and the importance of the activity of the deposited metal toward oxidation. For Hf and Cr, where two-dimensional growth occurs initially, a strong interface reaction is deduced from x-ray photoelectron spectroscopy (XPS). For Cu, which grows in three-dimensional islands, there is no indication of an interface reaction.[4]

We have now investigated the growth of Pt on the TiO_2(110) surface in some detail. Our motivation has been threefold. First of all we wanted to verify and check the general conclusions derived from the previous studies and to put them on a broader basis. Second, the system Pt/TiO_2 is of significant technological interest and a detailed understanding is therefore of general importance. Third, we were interested in the influence of molecules on the growth mode of metals. To keep things simple, we wanted to start out with a small molecule with well-known properties, namely, carbon monoxide (CO). Due to the large binding energy for CO on Pt, we expected that the growth mode of Pt might be affected if the evaporation were performed in the presence of CO.

Previous studies of Pt/TiO_2 using similar experimental techniques were mostly devoted to the interaction of Pt crystallites with a TiO_2 substrate.[8–10] There is extensive literature dealing with the preparation and thermal pro-

0163-1829/95/51(4)/2427(13)/$06.00

cessing of Pt/TiO_2 catalysts, i.e., Pt supported on high area TiO_2. After annealing Pt/TiO_2 catalysts in a reducing atmosphere, the chemisorption and catalytic properties change, which has been attributed to a strong metal-support interaction (SMSI).[9] Hence the study of the thermal stability of ultrathin metal films deposited on TiO_2 is another important topic. However, our study of this still controversial behavior will be the subject of a separate paper.[11] On the other hand, little is known about the growth of ultrathin platinum films on $TiO_2(110)$. In particular, while the SMSI behavior has been studied using low-energy ion scattering (LEIS) measurements,[8] no study of the growth using this technique has been reported. So the present article focuses on the growth mode at the early stages of Pt on $TiO_2(110)$, in ultrahigh vacuum as well as in presence of carbon monoxide.

In the following we first provide some details on the experimental setup in Sec. II and then present the experimental results in Sec. III. In Sec. IV the data are discussed and finally a summary is given in Sec. V.

II. EXPERIMENT

The experiments have been carried out in a UHV system with a base pressure of $\sim 1.3\times10^{-10}$ Torr, which has been described in detail elsewhere.[12] Briefly it is equipped with an x-ray source (Al $K\alpha$, Mg $K\alpha$) and a hemispherical analyzer (100 mm radius) for XPS, a quadrupole mass spectrometer for residual gas analysis, a retarding field display optics for low-energy electron diffraction (LEED), and a differentially pumped ion gun for sputtering. This ion gun in combination with the hemispherical energy analyzer is also used for LEIS experiments. These experiments are performed at a fixed scattering angle of 135° and 1-keV $^4He^+$ ions at an ion fluence per measurement lower than 10^{14} ions/cm^2.

The sample, a TiO_2 single crystal with (110) orientation, is mounted on an *XYZ* Rotary manipulator. It can be heated by radiation and by means of electron bombardment using a W filament mounted behind the sample. The crystal temperature is measured using a tungsten/rhenium thermocouple spotwelded onto the Ta case that holds the sample. The sample is cleaned by Ar^+ bombardment, followed by annealing in vacuum and oxygen to restore the surface stoichiometry (for details see Ref. 1). The Pt films are deposited using a shielded liquid-nitrogen-cooled metal source, through thermal evaporation from a small (2×2 mm^2) Pt foil spotwelded to a tungsten filament, at deposition rates of ~0.5 Å/min. During the evaporation the pressure in the chamber may increase on average by $(0.5-3)\times10^{-10}$ Torr; this can lead to a small contamination of the deposited layers for the longest time of evaporation, characterized by a small (a few percent) underestimation of the Pt LEIS signal. XPS C 1*s* spectra showed typically no indication of contamination with carbon. The sample temperature remains unchanged to within ±3 K. The average layer thickness is monitored using a quartz crystal monitor. The thicknesses given in this article are averaged thicknesses, by assuming uniformly thick films with the Pt bulk density 21.4 g/cm^3. This gives an average distance between layers of about 2.5 Å, a value that is slightly greater than the distance between (111) planes, 2.26 Å.[13] The latter will be taken hereafter as the average thickness of one "atomic monolayer."

III. RESULTS

A. Growth mode of Pt on $TiO_2(110)$

To investigate the growth mode of Pt on the $TiO_2(110)$ surface we have performed LEIS and XPS measurements for deposited layers of increasing average thickness θ_A. Since LEIS is extremely sensitive to the composition of the topmost layer,[14] the intensities of the substrate signal (Ti and O) and the overlayer signal (Pt) are proportional to the coverage of these elements in the top layer. Furthermore, we assume that the ion scattering yields of He^+, which are different for each element, are constant during Pt deposition, based on previous studies.[1,4–6] The LEIS spectra for increasing average Pt coverage are depicted in Fig. 1. The bottom spectrum (a) represents the spectrum of the clean, stoichiometric surface with characteristic peaks at 760 and 420 eV that are attributed to the Ti and O atoms in the top surface layer. Upon Pt deposition an additional peak develops in the LEIS spectra at 980 eV that is assigned to the Pt atoms adsorbed onto the $TiO_2(110)$ surface. (The high-energy shoulder on the Pt peak is due to ion gun focusing effects and does not affect the conclusions.) The intensity of the Ti (or O) and Pt peaks corresponds to the fraction of uncovered and Pt-covered surface, respectively. In Fig. 2 the intensities (peak areas) of the Ti and Pt LEIS peaks are depicted as a function of average Pt coverage. With increasing coverage the intensity of the Ti and O peaks decreases and simultaneously that of the Pt peak increases. The decrease of the Ti and O peaks with coverage occurs rather slowly: at an average Pt coverage of 3 Å, which is slightly more than one monoatomic Pt layer, the intensity of the Ti peak is still 70% of its original value, indicating that only 30% of the surface is covered with Pt islands. At an average coverage of ~6 Å the signal is reduced to

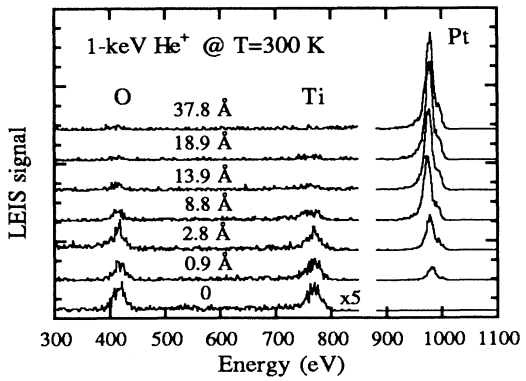

FIG. 1. LEIS spectra for $Pt/TiO_2(110)$ for average Pt coverages between 0 and 37.8 Å deposited at room temperature using 1-keV He^+ ions.

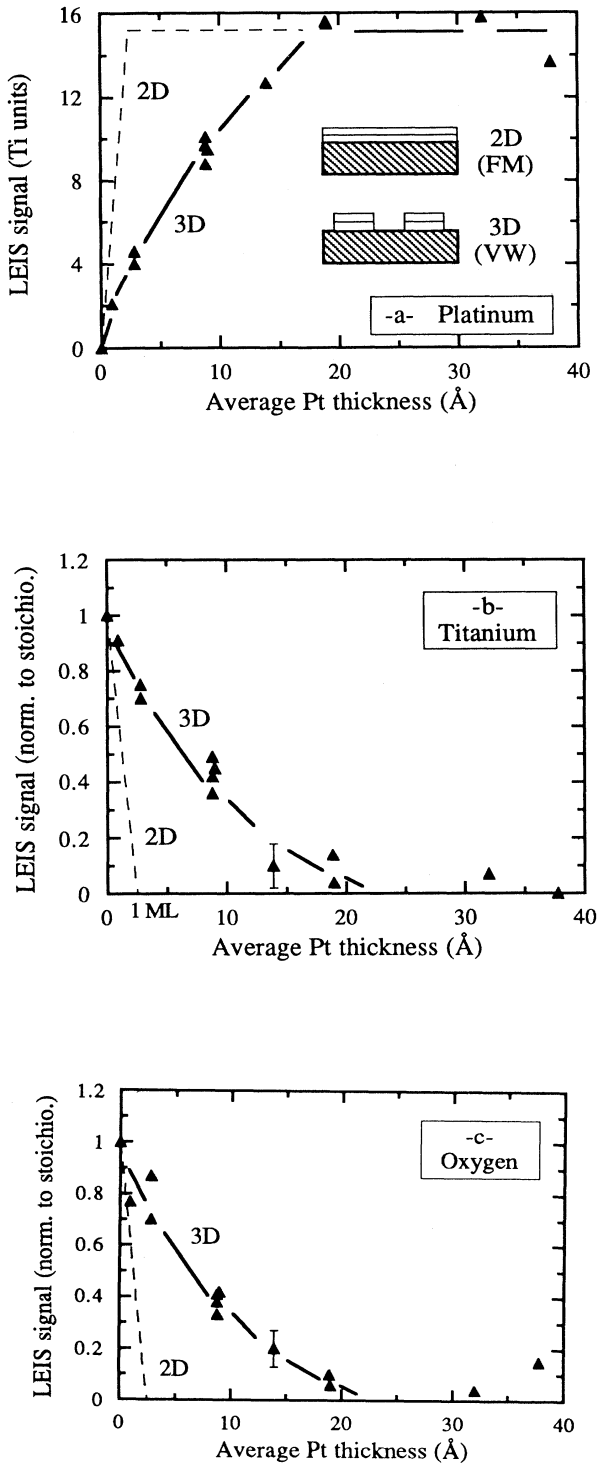

FIG. 2. Areas below each LEIS peak are shown as functions of Pt average thickness: (a) platinum, (b) titanium, and (c) oxygen. Pt and Ti values are normalized to the Ti value of the stoichiometric surface; O is normalized to its respective stoichiometric value. Thick lines are guides for the eye. The dashed lines indicate the behavior expected for two-dimensional growth as schematically depicted in the top of the inset in (a). The observed growth mode is three dimensional.

50% and only at an average coverage of about 25 Å the Ti signal (and also the O signal) disappears and the Pt signal reaches a saturation value. This behavior is indicative of growth of Pt in three-dimensional islands on the TiO_2(110) surface. For truly two-dimensional (layer-by-layer) growth one would expect the complete disappearance of the Ti signal and the saturation of the Pt signal at an average coverage that corresponds to a monoatomic layer ($\sim$2.5 Å). Note also that the normalized Pt intensity I_{Pt} is in good agreement with $1-I_{Ti}$. This confirms the assumption of the constant survival probability of He^+ ions.

B. Investigation of surface reactivity

Additional information on the growth of the Pt films can be derived from Ti $2p$ and Pt $4f$ XPS spectra. The spectra have been collected at two emission angles, namely, close-to-normal emission ($\sim$10° off the surface normal) and grazing emission ($\sim$70° with respect to the surface normal). Due to their short attenuation length (10–20 Å), the escape depth of the photoelectrons is limited to the top few atomic layers for grazing emission, whereas for angles close to the surface normal a deeper region normal to the surface contributes to the measured signal. The spectra have been collected using Al $K\alpha$ radiation with the pass energy of the analyzer set to 20 eV.

In Figs. 3(a) and 3(b) the Ti $2p$ and Pt $4f$ XPS spectra are depicted for increasing average Pt coverage, respec-

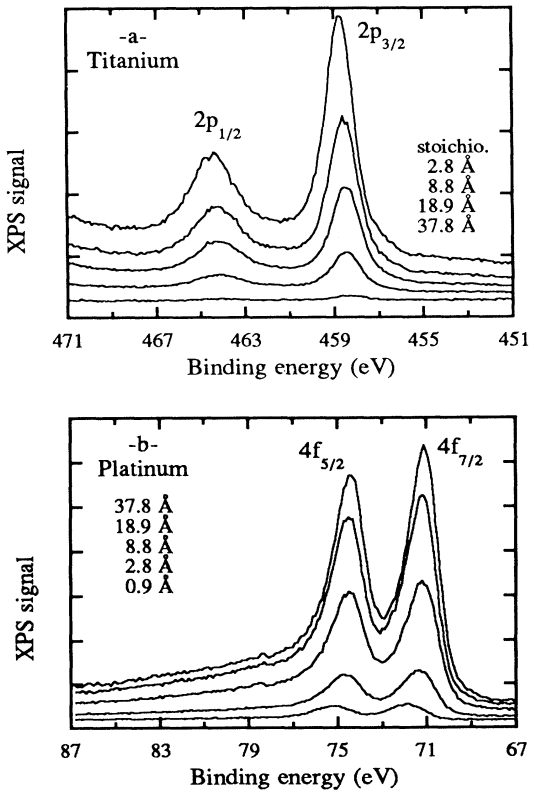

FIG. 3. XPS spectra of (a) Ti $2p$ and (b) Pt $4f$ for a series of Pt thicknesses between 0.9 and 37.8 Å, detected 10° off surface normal. Layers were deposited at room temperature.

tively. The Ti $2p$ spectra (a) are characteristic of the Ti^{4+} state of the stoichiometric $TiO_2(110)$ surface with the Ti $2p_{1/2}$ and $2p_{3/2}$ lines at binding energies of 464.4 and 458.6 eV, respectively. As one would expect, the intensities of the Ti $2p_{1/2}$ and $2p_{3/2}$ photoemission lines decrease with the average thickness of the Pt layer. At the same time emission from the Pt $4f_{5/2}$ and $4f_{7/2}$ levels develops at binding energies of 74.4 and 71.2 eV, respectively. As displayed in Fig. 4, the Pt $4f$ binding energy decreases by about 0.7 eV during the early stages of the layer growth, to reach the bulk value at around three atomic monolayers. The higher binding energy at low coverage can be interpreted as resulting from the emission from small Pt islands. As the islands grow in size, a bulklike situation is reached, electron screening becomes more efficient, and the electronic environment becomes more metallic. This evolution is in good agreement with a previous observation by Tamura *et al.*[15] However, we find a smaller amplitude for the overall shift: 0.7 eV as compared with 1 eV. This may be due to sample charging in the work of Tamura *et al.*[15] A similar core-level shift has also been reported for $Cu/TiO_2(110)$.[5] The energy shift is larger in the Pt case and the bulk value is reached at a higher average coverage than for Cu: three atomic monolayers instead of one. This may result from a more three-dimensional growth in the case of Cu, where the formed islands have a larger diameter for an equivalent average thickness, which means an atomic environment closer to that of the bulk.

Meanwhile no significant shifts (within ± 2.0 eV) in the energetic positions of the Ti $2p$ and O $1s$ lines are observed with increasing coverage. This indicates that no band bending due to Pt adsorption takes place and also suggests that there is little or no interface reaction at the Pt/TiO_2 interface. This conclusion is further strengthened by the fact that the Ti $2p$ XPS spectra show no indication of the formation of a reduced $Ti^{\delta+}$ species ($0 \leq \delta < +4$). The formation of such species is characterized by the observation of additional peaks in the Ti $2p$ XPS spectra at the low-binding-energy side of the spectrum. Such features are observed for nonstoichiometric surfaces, sputtered surfaces, or after an interface reaction between the deposited metals and the substrate. This interface reaction can occur immediately upon deposition as has been observed, e.g., for Hf,[7] for Fe,[6] or after annealing of the deposited metal layer to an elevated temperature.

The intensities (peak areas) of the Ti $2p$ and Pt $4f$ photoemission lines as a function of average thickness are depicted in Figs. 5(a) and 5(b), respectively. The spectra for close-to-normal and grazing emission are normalized such that for the stoichiometric surface the Ti $2p$ signal for both geometries is identical. This normalization is necessary because the measured intensity depends on the experimental geometry. The comparison of the Ti $2p$ spectra for the two experimental geometries reveals that for grazing emission the intensity decreases faster with coverage than for close-to-normal emission: For 70° the signal is reduced to 50% at an average Pt coverage of ~4 Å, whereas at 10° this occurs only at approximately twice that coverage. The comparison to the corresponding curve for the ion scattering data in Fig. 2 shows that the curve for the LEIS intensities (50% at 6 Å) lies in between the curves for the Ti $2p$ XPS spectra for close-to-normal and grazing emission. The intensities of the Pt $4f$ peaks increase with increasing average thickness; the ini-

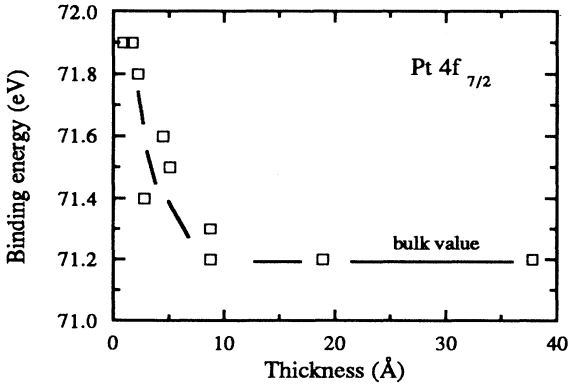

FIG. 4. Pt $4f_{7/2}$ binding energy as a function of Pt coverage on the stoichiometric $TiO_2(110)$ surface. The bulk value is rapidly reached at a thickness of about three atomic monolayers, after an initial decrease.

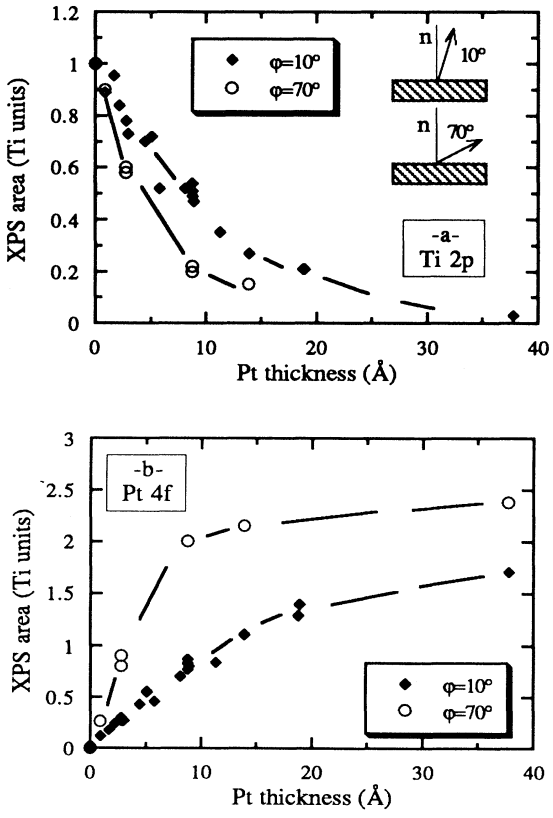

FIG. 5. XPS peak areas are plotted as functions of Pt coverage: (a) Ti $2p$ and (b) Pt $4f$. The filled diamonds (♦) refer to electrons detected close to normal emission ($\varphi = 10°$), whereas open circles (○) correspond to electrons emitted at grazing angles ($\varphi = 70°$). Lines are guides for the eye.

tial increase is steeper for the grazing emission angle, which is consistent with the faster decrease of the Ti 2*p* signal in this geometry. Interestingly, the intensities for the two geometries are not identical for very thick layers, as one would expect at first sight. This behavior is attributed to different reasons: First of all, the intensity for close-to-normal emission probably has not completely reached the saturation value; second, the lower intensity for close-to-normal emission could be due to a forward-scattering minimum (see the angle-resolved XPS data at $-10°$ described in Sec. III D below). Finally, it should be noted that for the Ti 2*p* as well as for the Pt 4*f* intensities no breaks were observed as a function of coverage, which is consistent with the three-dimensional growth mode that has been derived from the LEIS data.

C. Effect of substrate temperature on Pt film growth

To investigate the influence of the substrate temperature on the growth mode of Pt/TiO_2(110), we have measured LEIS spectra for substrate temperatures of 160 and 420 K, in addition to the spectra obtained at 300 K. The intensity of the Ti peak in the LEIS spectra is depicted in Fig. 6. It is observed that the decrease of the Ti signal with Pt coverage depends significantly on the substrate temperature. At a substrate temperature of 160 K, the signal (open circles) initially decreases approximately two times faster with Pt coverage than at room temperature (300 K, filled diamonds). For a substrate temperature of 420 K the decrease of the Ti signal (open triangles) is somewhat slower than at room temperature. Measurements at temperatures higher than 420 K were not performed since for temperatures ≥ 450 K a reaction between the TiO_2(110) substrate and the deposited Pt atoms occurs, as is concluded from the subsequent annealing of room-temperature-deposited layers to elevated temperatures. This behavior is connected to the SMSI properties exhibited by the Pt/TiO_2 system.[16,9] Upon annealing, an encapsulation of the Pt islands with a reduced $Ti^{\delta+}$ species ($0 \leq \delta < +4$) occurs, with the degree of reduction depending on the thickness of the Pt layer. However, this behavior is beyond the scope of the present work and will be the subject of a separate paper.[11]

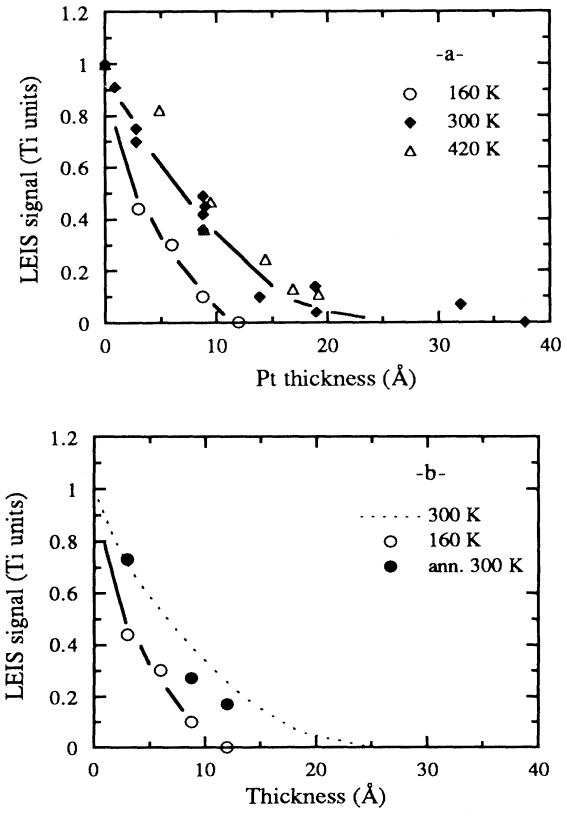

FIG. 6. (a) Deposition of Pt on TiO_2(110) at 160 (○), 300 (◆), and 420 (△) K. Ti LEIS intensity is plotted versus Pt thickness. Lines are guides for the eye. (b) The LEIS Ti signal (○) almost recovers the 300 K value (dashed line), when the 160 K deposited layers are annealed at 300 K (●).

From the fact that the Pt 4*f* intensities are almost identical for the 300 and 160 K layers for the same value of average Pt thickness, we believe that the amount of Pt on the surfaces is the same for both cases, as is expected. The shape of the XPS Pt 4*f* signal does not depend on the sample temperature nor on the emission angle (10° or 70°). Thus the chemical and electronic environments of the first Pt atoms in contact with the TiO_2 surface are independent of adsorption temperature.

In a next step we annealed the Pt layers deposited at 160 K to room temperature (300 K) for 15 min. The resulting data points are depicted in Fig. 6(b) (filled circles), along with the data after deposition at 160 K (open circles) and the data for deposition at room temperature (dashed line). The annealing procedure leads to a significant increase of the Ti LEIS intensity to values similar or close to those obtained for deposition at room temperature. This is an indication that the Pt atoms adsorbed on the TiO_2 surface at low temperature form islands that do not reach thermodynamic equilibrium. If the thermally activated diffusion of the adatoms is sufficient, the energetic balance leads the Pt crystallites to coalesce into thicker islands. This behavior is an example of the influence of the kinetics on the growth mode. It must thus be emphasized that the apparent growth does not necessarily give unambiguous information on the respective strength of metal-metal and metal-oxide bonds.

D. Structural investigations

To obtain information on the geometric structure of the deposited Pt layers we have investigated thick (> 18-Å average thickness) room-temperature deposited layers with LEED and angle-resolved XPS measurements. The LEED measurements showed a hexagonal pattern with broad diffraction beams. This indicates the growth of crystallize with fcc structure and (111) orientation. The crystallites are azimuthally oriented with the [1$\bar{1}$0] direction of the crystallites parallel to the [001] azimuth of the substrate. The relatively broad diffraction beams are probably due to the small size of the crystallites and the low degree of long-range ordering, both being a result of the relatively low deposition temperature of 300 K. For

the angle-resolved XPS measurements the sample was rotated in steps of 2° around the surface normal, thereby changing the polar angle with respect to the electron analyzer. The corresponding results are depicted in Fig. 7(a) for average thicknesses of 19 and 32 Å. The spectra show pronounced maxima along polar angles of $\varphi=0°$, 19°, and 34° (vertical arrows). The peaks develop sharper as the Pt layer becomes thicker. The sharp decrease of the signal amplitude below −40° and beyond 10° results from instrumental effects. We checked that the corresponding XPS background does not display any sharp variation in the displayed range of angles, so that this effect does not modify the results.

The positions of the XPS maxima correspond to dense crystallographic directions and correlate very well with the angles of the forward-scattering directions of a (111) fcc surface, $\varphi=0°$, 20° and 35° [see Fig. 7(b)] with the azimuthal orientation as derived from LEED. These results indicate well-defined short-range order in the deposited Pt layers and are also in very good agreement with the above conclusions derived from the observed LEED pattern.

As shown on Fig. 7(b), two equivalent orientations are possible for the fcc (111) geometry, which leads to the existence of two domains rotated by 180° with respect to each other, depending on which hollow site the second layer is adsorbed (sequences *ABCA*... or *ACBA*...). According to the data of Fig. 7(a), we can deduce that both orientations are present for this 32-Å Pt layer, since we may interpret the peak at −20° as coming from domain I [top of Fig. 7(b)] and the peak at −34° as coming from domain II [bottom of Fig. 7(b)].

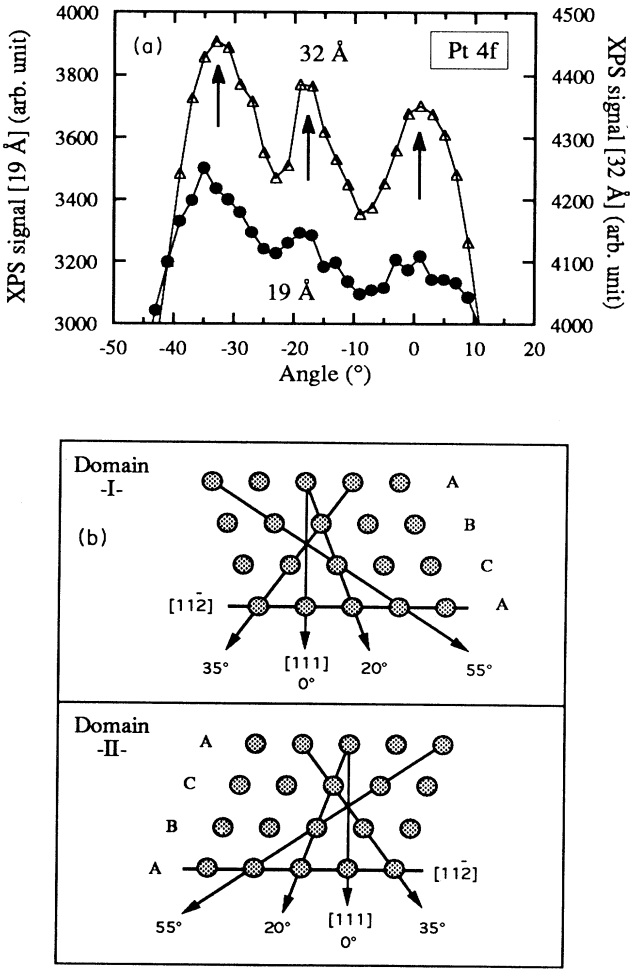

FIG. 7. (a) Angle-resolved XPS for 19° (●) and 32° (△) -thick platinum layers. The Pt 4*f* area is plotted versus the off-normal emission angle. (b) This schematic of fcc (111) geometry indicates the close-packed directions where the XPS signal is expected to be maximum (arrows). Two equivalent orientations are possible for this geometry, which leads to the existence of two domains rotated by 180° with respect to each other, depending on which hollow site the second layer is adsorbed (sequences *ABCA*... or *ACBA*...).

E. Evaporation in the presence of carbon monoxide: Evidence for a surfactant effect

We have investigated a possible surfactant effect of CO in the growth mode of Pt on the TiO_2(110) surface. For this study we have evaporated (at a rate of 0.5 Å/min) Pt in a CO atmosphere of 10^{-6} Torr, with the substrate at room temperature as well as at 160 K, and measured the LEIS and XPS spectra after deposition. At 300 K no CO adsorption occurs on the TiO_2 surface, as concluded from XPS (no C 1*s* emission) and from LEIS. However, CO readily adsorbs on Pt at this temperature with a sticking coefficient close to unity.[17–20] At 160 K, CO is not expected to adsorb on titania.[21] Our XPS spectra indeed showed no evidence of adsorbed CO on the clean TiO_2 surface. However, some decrease (typically less than 10%) of the LEIS Ti peak may occur after exposure to CO at this temperature: We believe that this is due to contamination from residual water; however, the effect is significantly smaller than the observed surfactant effect, as we will see in the following. The experimental conditions correspond to impingement rates of CO and Pt of $\sim 10^{15}$ and $\sim 3\times 10^{12}$ particles/cm^2 sec, respectively.

Figure 8 displays the LEIS spectra of a 5.7-Å layer deposited onto TiO_2(110). The bottom curve shows the spectrum for the stoichiometric support. The middle curve displays a decrease in O and Ti intensities as Pt is deposited in presence of 10^{-6} Torr of CO, at room temperature. Note the very small intensity of the Pt peak, due to the masking by the adsorbed CO molecules on Pt. The top curve shows the peaks when the sample is annealed at 500 K; the peak amplitudes will be discussed in the following paragraph. First, let us focus on Figs. 9(a) and 9(b), where we have depicted the intensity of the Ti and the Pt LEIS signal as a function of average Pt thickness. For comparison the results for evaporation without the presence of CO are indicated as a dashed line. The Ti signal in the presence of CO decreases significantly faster than without CO; the observed difference is not as pronounced as for the adsorption temperature of 160 K, but is clearly visible. Independent of coverage, no significant Pt LEIS signal is observed, which indicates that the Pt atoms in the top layer are blocked by the adsorbed CO

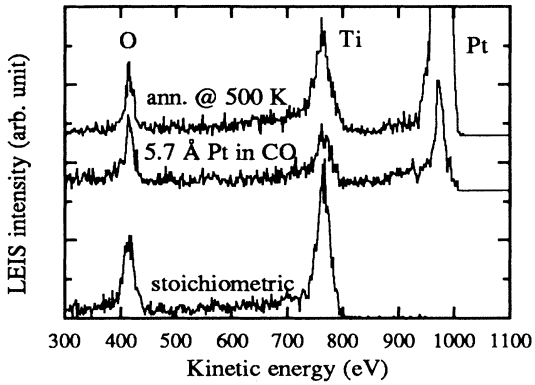

FIG. 8. LEIS spectra of the 1-keV He^+ ions for a 5.7-Å Pt layer on TiO_2(110). The lower curve corresponds to the stoichiometric TiO_2 surface, the middle curve to a 5.7-Å Pt layer deposited in the presence of 10^{-6} Torr of CO, at room temperature. The upper curve shows the reappearance of the Pt signal after the sample was annealed at 500 K for 3 min, in order to desorb CO.

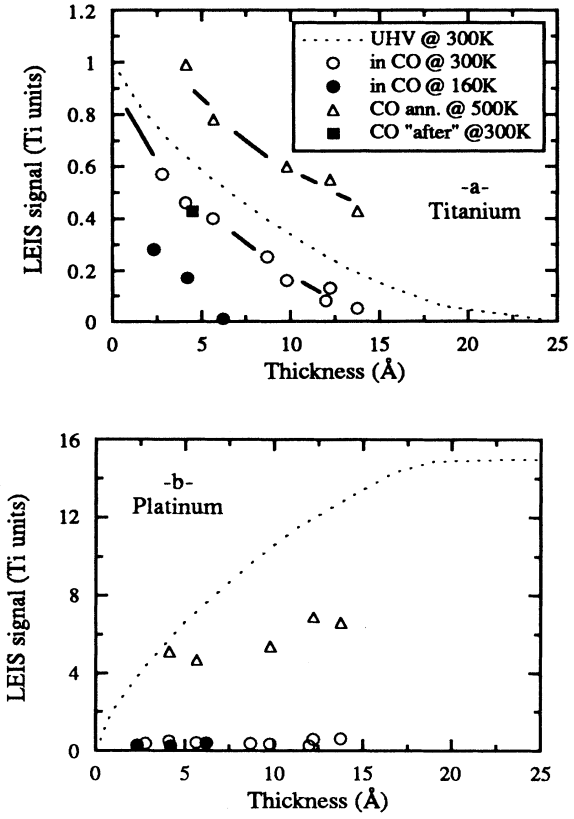

FIG. 9. Deposition of Pt on TiO_2(110) in the presence of 10^{-6} Torr of CO. The LEIS intensities of (a) Pt and (b) Ti are displayed as functions of Pt thickness. The open circles (○) correspond to deposition at 300 K and the filled circles (●) at 160 K. Also shown is the intensity of the Pt signal (△) after annealing at 500 K for 3 min: the signal does not recover its UHV-deposited amplitude and the Ti signal reaches values higher than the UHV values, due to a SMSI effect (see text). The filled square indicates the LEIS signal when Pt is exposed to CO *after* deposition in UHV.

molecules [Fig. 9(b)].

The deposition of Pt in the presence of gaseous CO onto TiO_2 at 160 K leads to an even better spreading of Pt, as indicated by the filled circles in Fig. 9(a). The TiO_2 support is completely covered at a coverage of approximately 2.5 monolayers (ML) of Pt ($\cong$6 Å), in contrast to the UHV case at room temperature, where the support disappears only above 6 or 7 ML (dotted curve).

It is worth noting that the CO-induced spreading is also observed when exposure to CO is performed *after* deposition in UHV at room temperature. This is indicated in Fig. 9(a) by the filled square. The decrease of the free titania surface area is of the same amplitude, as deduced from the reduction of the Ti contribution to the LEIS signal. The total CO exposure was about 7 L (1 L = 10^{-6} Torr sec) for this experiment.

The next experimental step consists of desorbing the CO overlayer from the Pt islands, to study the stability of the wetting effect when the surfactant is removed. We proceeded by annealing the sample at 500 K for 3 min; this treatment is sufficient to cause desorption of the CO monolayer. The upper curve of Fig. 8 shows the reappearance of a large Pt signal after annealing the sample. The triangles in Figs. 9(a) and 9(b), in the case of the deposition at 300 K, show the influence of annealing on LEIS intensities. First, the Pt LEIS signal does not fully recover its UHV-deposition value when the CO molecules are desorbed, although a substantial increase is observed. Second, the Ti LEIS signal increases toward values that are *beyond* the UHV curve. This behavior is related to the strong metal-support interaction effect,[8,16] caused by the encapsulation of the Pt islands by a TiO_x suboxide, as we will report elsewhere.[11] It is therefore not possible to distinguish the effect of removing the adsorbate from that of the oxide reactivity with the Pt overlayer.

The fact that CO is adsorbed on the Pt atoms is also confirmed by the C 1*s* XPS spectra, as displayed by the upper curve in Fig. 10, for a 12.2-Å Pt layer. After the

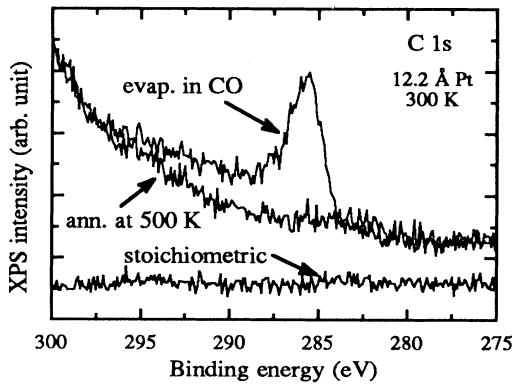

FIG. 10. XPS C 1*s* spectra are shown for a 12.2-Å platinum layer, deposited on TiO_2(110) in the presence of 10^{-6} Torr of CO, at room temperature. Unlike the clean stoichiometric surface (lower curve), a clear peak is observed at a binding energy consistent with a molecularly adsorbed CO (higher curve). When the sample is annealed at 500 K for 3 min, the CO molecules are desorbed (middle curve).

deposition of Pt in the presence of CO, a pronounced peak appears at a binding energy of 285.5 eV that is attributed to molecularly adsorbed CO. The peak is suppressed by annealing at 500 K (middle curve in Fig. 10). The high-energy tail, of lower amplitude, can be interpreted as a satellite structure due to charge transfer satellites and "shake-up" states.[22]

The variation of the C 1*s* intensity as a function of Pt coverage is depicted in Fig. 11 for Pt deposition in a CO atmosphere at substrate temperatures of 160 K (filled circles) and 300 K (open circles). In addition, the result for postdosing CO onto a Pt layer deposited under UHV conditions is indicated (filled square); similar to the LEIS data of Fig. 9(a), the latter value is close to the CO-deposited case. For both sample temperatures, the curves display an initial increase with coverage. At 300 K, the CO contribution to the XPS signal seems to saturate at an average Pt thickness (10–12 Å) that roughly corresponds to the coverage at which the TiO_2 substrate is fully covered with Pt. For 160 K deposition, the amount of adsorbed CO at a given average Pt thickness is larger than for 300 K deposition. This can result from two factors acting in the same direction. On the one hand, the Pt islands are flatter at 160 K, since the same amount of Pt atoms cover a larger fraction of the TiO_2 substrate, which means that there are more adsorption sites available to CO. Indeed, the ratio of C 1*s* intensities at 300 and 160 K roughly scales (e.g., around 4 Å) with the ratio of the fractions of the surface covered with Pt, as obtained from [1-LEIS(160)]/[1-LEIS(300)] in Fig. 9(a). On the other hand, the CO saturation coverage (i.e., the occupancy of adsorption sites as well as the number of available sites) should increase as the temperature is lowered.[17–20] This effect should dominate in the regime of high Pt coverages, where the surface is completely covered and the number of CO adsorption sites is similar for both deposition temperatures. In the low coverage regime of Pt both effects should contribute to the observed behavior.

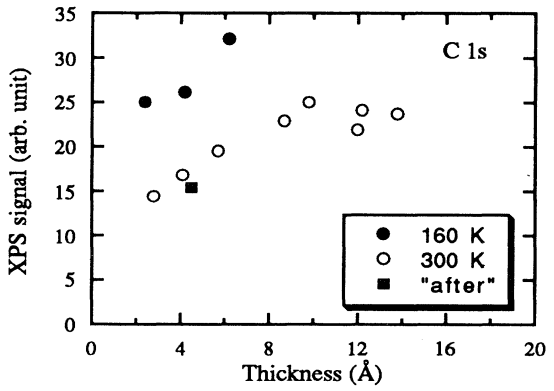

FIG. 11. The amplitude of the main XPS C 1*s* peak is plotted as a function of the Pt thickness, for the two deposition temperatures in the presence of 10^{-6} Torr of CO: 300 K (○) and 160 K (●). At a given temperature, the overall increase corresponds to a larger adsorption area as Pt grows. At a given average thickness, the larger signal at low temperature corresponds to a maximization of islands area, due to their flattening. The filled square indicates the result of exposing a UHV-deposited 4.5-Å layer to 7 L of CO.

Finally, the adsorption of carbon monoxide on top of the platinum islands gives rise to an interesting electronic effect. This is evidenced in Figs. 12(a) and 12(b), which display the XPS Ti 2*p* and Pt 4*f* spectra, respectively, for 8.8-Å Pt layers deposited in UHV or in the presence of CO. While the titanium line does not show evidence of a significant core level shift (within 0.1 eV), as compared with the stoichiometric situation, on the contrary, the platinum line shows a shift of about 0.6 eV toward high binding energies, for the CO-evaporated layer as compared with the UHV-evaporated one [horizontal arrows in Fig. 12(b)]. The slight decrease of the Pt 4*f* signal is due to the attenuation of the photoelectrons by the CO layer (the measurements were performed at grazing emission).

IV. DISCUSSION

A. The growth mode

We begin by analyzing the growth mode of Pt on the TiO_2(110) surface for deposition at room temperature.

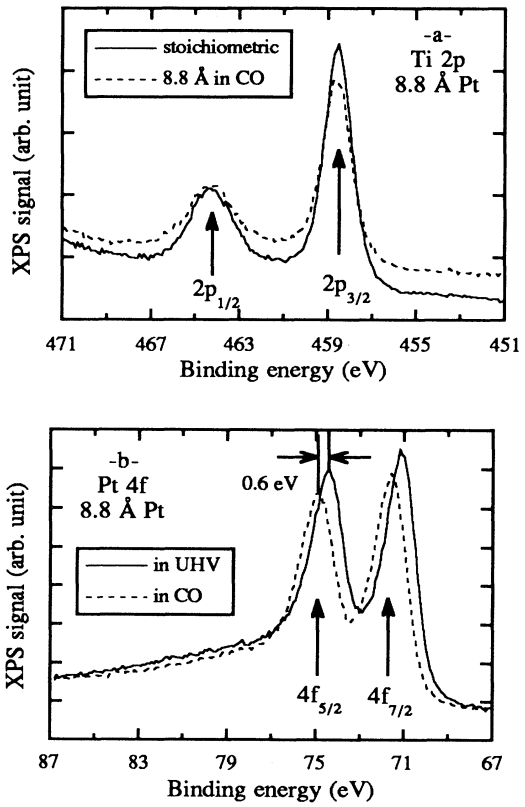

FIG. 12. (a) Ti 2*p* and (b) Pt 4*f* XPS spectra displaying the chemical shifts associated with the adsorption of CO, for a 8.8-Å-thick Pt layer, deposited at 300 K. No significant shift is observed for Ti, while a 0.6-eV core-level shift toward higher binding energies is observed for the Pt layer deposited in the presence of CO (dashed curve) as compared with a layer deposited in UHV (plain curve). All curves were measured at a grazing emission (70° off the sample normal).

The LEIS spectra indicate a growth of three-dimensional Pt islands. At an average coverage θ_A of 2.8 Å, which corresponds to slightly more than one monoatomic Pt layer, the Ti LEIS signal is reduced to 72±5%, which means that only 28% of the TiO_2 surface is covered with Pt; for an average coverage of $\theta_A = 8.8$ Å the LEIS signal is reduced to 40±5%, i.e., 60% of the surface is covered by Pt. From the average thickness θ_A of the deposited Pt films and the covered surface area, we can derive an average thickness of the three-dimensional Pt islands; for the two examples given above we obtain values of 10 Å for $\theta_A = 2.8$ and 15 Å for $\theta_A = 8.8$ Å. Some further information on the lateral width of the islands can be obtained from the Ti 2*p* XPS spectra, in particular for grazing emission angles ($\varphi = 70°$). As mentioned above in Sec. III B, the Ti 2*p* XPS signal disappears for increasing Pt coverage at a steeper slope than the Ti LEIS signal. This observation is surprising at first sight since one would expect that the XPS signal should disappear slower due to the fact that it is composed of contributions from electrons from the uncovered surface plus electrons from the covered surface with the latter being damped exponentially by the Pt layer. For average thicknesses ≥ 10 Å, the contribution from electrons from regions beneath the Pt layer should be negligible for grazing emission. For close-to-normal emission Ti 2*p* electrons from beneath the Pt islands can contribute since their escape depth (normal to the surface) is about a factor of 3 larger than for grazing emission (70°). This is indeed the case since the Ti 2*p* XPS intensities for normal emission decrease slower than the LEIS signal. The fact that the Ti 2*p* signal for grazing emission is lower relative to the Ti LEIS signal can only be explained if we assume shadowing effects in the XPS experiment, as is schematically depicted in Fig. 13. Due to the height of the Pt islands a certain fraction of the uncovered TiO_2 surface is not "visible" to the detector at grazing emission angle. In other words, electrons from these areas of the bare surface are, depending on their path length through the Pt island, either completely absorbed or strongly reduced in their contribution to the measured signal. A similar shadowing effect may influence LEIS, but not as significantly as grazing angle XPS.

B. Considerations on the island shapes

In a zero-order approximation we can compare the XPS and the LEIS behavior to get a rough estimate of the average island sizes by assuming a cubic shape for the islands and furthermore only taking those bare areas into account from which electrons can directly reach the detector. Based on these assumptions we obtain average island characteristic sizes of 70 and 170 Å for average thicknesses of 2.8 and 8.8 Å, respectively. These numbers are certainly only an upper limit for the average island size, since in this simplified approximation all corrections toward a more realistic model lead to smaller island sizes. Among these corrections are the neglect of shadowing effects in LEIS (where an incidence angle of 35° with respect to the surface normal was used), a more realistic shape of the islands (e.g., hemispheres), and the fact that at the edges of the islands the substrate signal will not be completely attenuated by the islands, but will contribute to a certain extent.

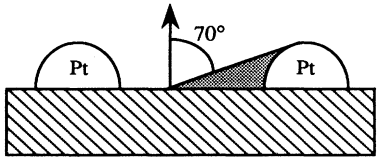

FIG. 13. Schematic drawing of the shadowing effects at grazing emission ($\varphi = 70°$ off normal). A significant part of the support area can be masked by scattering or absorption of the emitted electrons by the Pt islands.

Nevertheless, we can try to progress beyond these limitations by considering a simple model for the island shapes, "flat island" versus "hemispherical islands," as developed by Diebold, Pan, and Madey.[5] The model considers either flat islands of constant height t, with a coverage θ being defined as $d = \theta t$, where d is the measured "average Pt thickness" (see the inset in Fig. 14), or hemispherical clusters of constant radius R and distribution n, such as $d = \frac{2}{3}\pi n R^3$ (not shown here). For each average thickness d, the island parameters are computed by assuming a simple relation for the XPS intensities of the adsorbate and the substrate, Pt and Ti [Figs. 5(a) and 5(b)]. The model equations for flat islands are[5]

$$\frac{I_{\text{ads}}}{I_{\text{ads}}(\infty)} = \theta \left[1 - \exp\left[-\frac{t}{\lambda_{\text{ads}}} \right] \right], \tag{1}$$

$$\frac{I_{\text{sub}}}{I_{\text{sub}}(0)} = 1 - \theta + \theta \exp\left[-\frac{t}{\lambda_{\text{sub}}} \right], \tag{2}$$

with the XPS intensities normalized, respectively, to the values of the thickest Pt film (37.8 Å), $I_{\text{ads}}(\infty)$, and to an uncovered stoichiometric support $I_{\text{sub}}(0)$. The attenuation lengths of the photoelectrons emitted from both the Pt clusters and from the substrate, λ_{ads} and λ_{sub}, are both chosen to be 8 Å, by similarity with Cu; these values were then confirmed by self-consistency of the calculation. In effect, summing Eq. (1) with Eq. (2) should give unity if both lengths are identical. This is indeed observed: Experimental XPS intensities of Figs. 5(a) and 5(b) ($\varphi = 10°$) add to 1.00±0.05 for the whole range of thickness. The computed island parameters are obtained by inserting the Pt intensities [data of Fig. 5(b), $\varphi = 10°$; normalized] in Eq. (1) and used to compare the Ti XPS intensity of Fig. 5(a) (at $\varphi = 10°$) with the calculated intensity, using Eq. (2). The same process is followed in the case of hemispherical clusters, with slightly more complicated equations.[5]

The results of the calculation for Pt is that both the flat island and the hemispherical island models give a satisfactory description of the XPS intensities (not shown). However, a difference occurs when we compute the LEIS intensities with the island parameters. The intensity

$I_{sub}^{ion}/I_{sub}^{ion}(0)$ is assumed to be equal to $1-\theta$, for flat islands, and to $1-\frac{3}{2}\pi nR^2$, for hemispherical islands. The result for the flat island case is displayed in Fig. 14: the computed LEIS intensity $1-\theta$ (triangles) and the thickness t (diamonds) are plotted as functions of the average thickness d. The scattering of calculated points reflects the experimental scattering in the intensity measurements. We find rather good agreement of the calculated LEIS intensity with the experimental data of Fig. 2(b) (dashed line in Fig. 14), except around the complete coverage, at $d \cong 20$ Å. In this region, the experimental LEIS intensity is expected to overestimate the actual coverage, due to shadowing effects. This is what is observed (LEIS intensity reaches zero before complete coverage). Thus the computed value of θ seems to be, at least, qualitatively correct. On the contrary, the hemispherical island model leads to a significant departure from the observed LEIS behavior: It predicts a complete coverage at an unphysical average thickness d of only 10 Å (not shown). The fact that significant shadowing effects are observed in the Ti XPS intensities is a strong indication that the islands have relatively steep edges, since otherwise smaller shadowing effects are expected. This is consistent with the flat island assumption. The thickness t is about 10 Å at low coverage, which is smaller than the calculated radius R of about 17 Å in the case of Cu;[4] this is consistent with a slower coalescence of smaller Pt crystallites at low coverage (see also the slower saturation of the Pt $4f$ core-level shift, Fig. 4). The flat island model reproduces the grazing angle XPS curves of Figs. 5(a) and 5(b) only qualitatively, because no shadowing effect is taken into account.

We have tested the flat island assumption by calculating the island parameters at the lowest temperature of 160 K. First, we find good agreement between the computed $1-\theta$ and the experimental Ti LEIS intensity (not shown); second, the calculated island thickness t at low coverage is noticeably smaller at 160 K than at 300 K (almost by a factor of 2). This means that for a given number of Pt atoms per island the islands must have a larger diameter at the lowest deposition temperature; this is consistent with the higher degree of wetting (complete coverage occurs at smaller average thickness) at low temperatures. At this point it is important to note that within our model we are not able to determine the *diameter,* i.e., the *lateral* dimensions, of the Pt crystallites. However, the curve fitting suggests that the height of the islands increases as temperature increases and thus that their lateral dimensions must decrease, by conservation of mass: the islands are *flatter* at lower temperature.

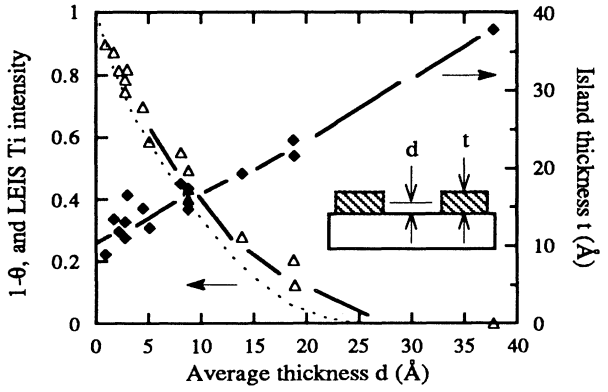

FIG. 14. Computed LEIS intensity, $1-\theta$ (△ symbols), and the island thickness t (◆, right scale), plotted as functions of the average Pt thickness d by assuming a simple flat island model for the distribution of Pt clusters, as depicted in the inset. All islands are supposed to have the same height t and θ is defined by $d=\theta t$. Thick lines are guides for the eye. The $1-\theta$ curve is compared with the experimental LEIS Ti curve (dotted line).

Now, let us come back to the angle-resolved XPS results, shown in Fig. 7(a). Our data can be compared with the $Cu/TiO_2(110)$ case, where more rounded angle-resolved XPS peaks were observed and only weak maxima were discernible.[4] This was interpreted by Pan *et al.* as resulting from the existence of equivalent domains of the Cu fcc (111) crystallites.[4] The superposition of the diffraction patterns from the two domains was believed to be responsible for the broad peaks for Cu. However, our Pt data display better resolved maxima (see also Ref. 15). The relative amplitude of the peaks is about 4% for Pt and less than 1–2 % for Cu.[4] The explanation of the observed differences between Pt and Cu could be manyfold: First, the degree of local ordering could be higher for Pt, leading to a more pronounced diffraction pattern; second, a possible azimuthal misalignment of the TiO_2 crystal could have led to a smearing out of the Cu features; third, the difference in kinetic energies between Cu $2p$ and Pt $4f$ photoelectrons (respectively 0.56 and 1.4 keV) could lead to somewhat sharper Pt features, since a higher energy could lead to more pronounced maxima; fourth, the emission from the $4f$ orbitals (Pt) should be more directional than the emission from p orbitals (Cu), which also could contribute to the more anisotropic scattering behavior for Pt. Furthermore, the difference in island shape [flat islands for Pt and hemispherical islands for Cu (Ref. 5)] could be an important factor. We believe that probably a combination of several of these factors is responsible for the more pronounced maxima in the Pt $4f$ photoelectron diffraction pattern.

C. Absence of interface reactivity on deposition

The energetic position and the shape of the Ti $2p$ and Pt $4f$ XPS spectra give no indication of a reaction of the adsorbed Pt islands with the substrate, independent of the average Pt coverage. The initial shift in the Pt binding energy (Fig. 4) is attributed to an electronic effect of the finite size of isolated clusters, due to the screening of the core-hole electrons by the electrons on neighboring atoms.[15,5] The screening is expected to increase as the crystallites grow in size, reaching a bulklike metallic situation. This leads to a decrease in binding energy. The bulk situation is reached for Pt at a higher average thickness than for Cu, which is consistent with different shapes for the respective crystallites: flat islands for Pt and hemispherical islands for Cu, which are found to grow at an earlier stage.[5]

The Ti $2p$ peaks at close-to-normal emission—where a contribution from the Ti species beneath the islands is ex-

pected to be significant—exhibit no shoulder or peak on the low-binding-energy side that would indicate the formation of a reduced species at the Pt/TiO_2 interface. If the deposited Pt layers are, however, annealed to temperature above 450 K, the formation of a reduced Ti species is observed that is attributed to a $Ti^{\delta+}$ (with $0 \leq \delta < +4$) layer on top of the Pt islands.[11]

D. Thermal stability of the ultrathin films

The variation of the substrate temperature between 160 and 420 K leads to a significant change in the growth behavior. As mentioned above, the Ti LEIS signal disappears significantly faster at a substrate temperature of 160 K, but is nearly restored to the value obtained for room temperature, if the low-temperature deposited Pt layer is annealed to room temperature. The stronger decrease of the Pt signal at low temperature is attributed to the lower diffusion rate of incoming Pt atoms on the TiO_2(110) surface. At low temperatures, the mobility of Pt atoms is reduced such that diffusion of Pt on the TiO_2 substate and from the substrate onto the Pt islands is strongly hindered. Due to the lower diffusion rate the Pt atoms cannot form large three-dimensional islands with large average thickness, but rather form a higher number of smaller islands with smaller average thickness. This way the same amount of Pt leads to a higher fraction of the surface being covered with islands. Upon annealing, by diffusion the smaller islands disappear and larger, thicker islands are formed. The fact that for the larger average island thicknesses the value of the room-temperature deposited layers is not completely reached by the annealing process is probably due to the fact that the annealing time was not long enough.

The comparison with the growth behavior of other metals (Cu, Fe, Cr, and Hf) on TiO_2 shows that the behavior of Pt is somewhere between the behavior of Cu and Fe. Similar to Cu, Pt grows in three-dimensional islands and no interface reaction occurs (for $T < 450$ K). On the other hand, the three-dimensional growth is not as pronounced as for Cu, where even at an average coverage of 30 Å one-third of the surface is uncovered; for Pt the surface is completely covered at this average coverage. For Fe the TiO_2 surface is already covered at lower average coverage (~ 10 Å) than for Cu, but there is some indication of an interface reaction upon adsorption.[4]

E. The surfactant effect of carbon monoxide

As shown in Figs. 8 and 9, CO has a noticeable influence on the growth mode of Pt onto the TiO_2(110) surface. The decay of the Ti peak in the LEIS spectra with increasing Pt coverage is significantly faster than without CO. Since CO does not adsorb on the bare TiO_2(110) surface, even at 160 K, this effect cannot be attributed, e.g., to a lower mobility of Pt on a partially CO-covered TiO_2(110) surface, but is rather due to the bonding interaction of CO to the platinum atoms in the top layers of the islands.

In the following, we propose a simple qualitative model that can account for the observed behavior. On the one hand, we know that Pt grows on the TiO_2(110) surface in three-dimensional islands. On the other hand, CO strongly chemisorbs molecularly with a high sticking probability (0.5–1.0), on polycrystalline Pt and on all the low index facets: (100), (110), and (111).[17–20] Depending on the crystallographic orientation of the surface, the binding energy is on the order of 1–1.3 eV per molecule. The system thus can gain energy by adsorbing CO molecules. This is reflected for instance in the XPS Pt 4*f* curve of Fig. 12(b): the 0.6-eV core-level shift may be attributed in part to a gain in binding energy. This gain could result from the energy balance between, on the one hand, the Pt/TiO_2 interfacial energy, which is not favorable to wetting of TiO_2 by Pt, or, on the other hand, the CO/Pt interfacial energy, which favors a maximum Pt surface area. Also, the presence of the CO adsorbate could reduce the surface core-level shift by making by the environment of the surface Pt atoms more bulklike.

The amount of energy that can be gained depends on the number of available adsorption sites on the surface, i.e., it is proportional to the number of surface atoms of the Pt clusters that grows on the TiO_2(110) surface. From simple arguments one can show that the number of surface atoms is larger for a broad, flat island as compared to a narrow, tall island, as exemplified in Fig. 15. Thus the driving force for the change in the growth behavior of Pt in the presence of CO is the higher number of Pt surface atoms for flatter islands that must compensate for the fact that in the absence of CO the growth of higher islands is energetically favored. An argument in favor of this geometric interpretation is provided by Fig. 11, which indicates that the number of CO molecules scales roughly with the percentage of covered support.

F. Comparison with other systems

A surfactant effect has been reported in the case of the homoepitaxy of Pt on Pt(111): The presence of oxygen during epitaxy induces a layer-by-layer growth, while Pt grows in a multilayer three-dimensional (3D) mode in UHV.[23] The authors claimed that the presence of O_2 reduces the barrier height for the motion of Pt adatoms across step edges, which facilitates the interlayer mass transport and thus the layer-by-layer growth. Unlike most other surfactants, such as As in the case of Si/Ge/Si(001) (Ref. 24) or Sb in the case of Ag/Ag(111),[25] gaseous surfactants such as O_2 or CO can be completely removed after the growth, which means important potential applications.

A surfactant effect has been reported in the case of CO in the growth of copper films on ZnO(0001)-O.[26,3] Ernst

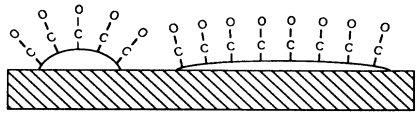

FIG. 15. Schematic drawing of the available number of CO adsorption sites for Pt islands containing the same number of Pt atoms, for different island shapes. For a given number of Pt atoms per island a flat island leads to a higher number of Pt surface atoms and correspondingly CO adsorption sites.

and co-workers performed similar LEIS and XPS measurements as in our present study. However, since Cu and Zn are not resolved in LEIS, the surfactant effect that they reported is based on the existence of a change in slope of the oxygen LEIS signal. The latter is somewhat ambiguous, since both the oxygen atoms of the oxide and the CO molecules contribute to the scattering of He^+ ions. Nevertheless, they conclude that CO adsorption can induce the Cu to redisperse from 3D islands to 2D islands even at 130 K. They interpret this effect in a way similar to our preceding arguments. They also invoke a kinetic explanation to account for the growth mode of metals onto oxides, claiming that the observed wetting cases may not result from mere energetic considerations, i.e., that metal-oxide bonds are stronger than metal-metal bonds, but rather from dynamic results.[3] The latter are reminiscent of the O_2/Pt/Pt(111) case, in which Esch *et al.* attributed the change in the growth mode to an oxygen-induced modification of the adatom diffusion properties.[23]

The same dynamic arguments can be used to interpret in the opposite way the better wetting that we observe at low temperature in Pt/TiO_2(110) [see Fig. 6(a)]. In such a case, Pt adatoms are not mobile enough at low temperature to form the energetically stable clusters that are found at room temperature. This does not mean that the metal-oxide interaction is modified with the temperature, but rather that kinetics play a more important role than energetics.

The filled square in Fig. 9(a) provides an example of the importance of energetics at 300 K. It suggests that in the case of the chemisorption of CO *after* formation of Pt islands, the latter yet redisperse to accommodate a larger Pt(111) area for optimizing the gain in adsorption energy. The energetics would thus play an important role in the process. Of course, this does not rule out a simultaneous change in the diffusion properties, caused by changes of the barrier height for the motion of Pt adatoms. The latter effect should be less important in the case of CO as compared to O_2: In effect, O_2 adsorbs dissociatively on Pt(111), whereas CO adsorbs molecularly. In the first case, the presence of atomic O should reduce the barrier height for the motion of adatoms. In the second case, it is worth noting that the gaseous surfactant can be easily removed after the growth, by heating the sample up to relatively low temperature—500 K—while a higher temperature—around 700 K—is necessary to associatively desorb O as O_2. However, as is indicated by our results, the presence of carbon monoxide is not sufficient to drive the growth of Pt on TiO_2(110) from three to two dimensions.

V. CONCLUSION

Platinum vapor deposited onto TiO_2(110) grows in three-dimensional islands. The growth mode depends on the temperature of the substrate. At low temperatures ($\sim$160 K) the surface is more uniformly covered than at room temperature with the size of the islands being smaller. Annealing of the low-temperature deposited layers leads to the formation of larger islands and an increase of the uncovered surface area; the fraction of the uncovered surface is very similar to those obtained by adsorption at room temperature. The formation of smaller islands at low temperatures is attributed to the low diffusion probability at these temperatures. Upon Pt deposition at $T < 400$ K, no reaction with the TiO_2 substrate occurs. The deposited Pt islands exhibit a (111) orientation with good local order and poor long-range order.

Carbon monoxide has a strong influence on the growth behavior and acts as a surfactant. If platinum is deposited in the presence of CO, a higher degree of the surface is covered by Pt islands, indicating a higher (though not complete) degree of wetting. The latter is still improved when the temperature of deposition is lowered. This behavior is correlated to the higher number of surface atoms and thus CO possible adsorption sites for flatter islands. Due to the larger binding energy of CO to Pt, it is energetically favorable to form islands with a larger number of adsorption sites, i.e., to form flat islands with a large fraction of the TiO_2(110) surface being covered.

ACKNOWLEDGMENTS

H.P.S. thanks the Deutsche Forschungsgemeinschaft and Rutgers University for financial support. F.P. acknowledges a CNRS-NSF Grant and financial support from Rutgers University.

*Permanent address: Experimentelle Physik II, Universität Würzburg, Am Hubland, D-97074 Würzburg, Germany.

†Permanent address: Laboratoire de Physique des Solides, Centre National de la Recherche Scientifique, Université de Paris-Sud, Bâtiment 510, F-91405 Orsay, France.

[1]J.-M. Pan, B. L. Maschhoff, U. Diebold, and T. E. Madey, J. Vac. Sci. Technol. A **10**, 2470 (1992).

[2]E. Bauer, Z. Kristallogr. Kristallgeom. Kristallphys. Kristallchem. **110**, 372 (1959).

[3]K. H. Ernst, A. Ludviksson, R. Zhang, J. Yoshihara, and C. T. Campbell, Phys. Rev. B **47**, 13 782 (1993).

[4]J.-M. Pan, B. L. Maschhoff, U. Diebold, and T. E. Madey, Surf. Sci. **291**, 381 (1993).

[5]U. Diebold, J.-M. Pan, and T. E. Madey, Phys. Rev. B **47**, 3868 (1993).

[6]J.-M. Pan and T. E. Madey, J. Vac. Sci. Technol. A **11**, 1667 (1993).

[7]L. Zhang, U. Diebold, and T. E. Madey (unpublished).

[8]D. J. Swyer, J. L. Robbins, S. D. Cameron, N. Dudash, and J. Hardenbergh, in *Strong Metal-Support Interactions,* ACS Symposium Series Vol. 298 (American Chemical Society, Washington, D.C., 1986), p. 21.

[9]For a review of SMSI effects, see G. L. Haller and D. E. Resasco, Adv. Catal. **36**, 173 (1989).
[10]Y. M. Sun, D. N. Belton, and J. M. White, J. Phys. Chem. **90**, 5178 (1986).
[11]F. Pesty, H.-P. Steinrück, and T. E. Madey (unpublished).
[12]B. L. Maschhoff, J.-M. Pan, and T. E. Madey, Surf. Sci. **259**, 190 (1991).
[13]N. W. Ashcroft and N. D. Mermin, *Solid State Physics* (Holt-Saunders, Tokyo, 1981).
[14]E. Taglauer, in *Ion Scattering Spectroscopies for Surface Analsyis,* edited by A. Czanderna and D. Hercules (Plenum, New York, 1991), p. 363.
[15]K. Tamura, M. Kudo, M. Owari, and Y. Nihei, Chem. Lett. **11**, 1921 (1986).
[16]S. J. Tauster, S. C. Fung, and R. L. Garten, J. Am. Chem. Soc. **100**, 170 (1978).
[17]G. Ertl, M. Neumann, and K. M. Streit, Surf. Sci. **64**, 393 (1977).
[18]G. Broden, G. Pirug, and H. P. Bonzel, Surf. Sci. **72**, 45 (1978).
[19]C. M. Comrie and R. M. Lambert, J. Chem. Soc. Faraday Trans. I **72**, 1659 (1976).
[20]D. M. Collins and W. E. Spicer, Surf. Sci. **69**, 85 (1977).
[21]M. A. Vannice, C. C. Twu, and S. H. Moon, J. Catal. **79**, 70 (1983).
[22]W. Wurth, D. Coulman, A. Puschmann, D. Menzel, and E. Umbach, Phys. Rev. B **41**, 12 933 (1990).
[23]S. Esch, M. Hohage, T. Michely, and G. Comsa, Phys. Rev. Lett. **72**, 518 (1994).
[24]M. Copel, M. C. Reuter, E. Kaxiras, and R. M. Tromp, Phys. Rev. Lett. **63**, 632 (1989).
[25]H. A. van der Vegt, H. M. van Pinxteren, M. Lohmeier, E. Vlieg, and J. M. C. Thornton, Phys. Rev. Lett. **68**, 3335 (1992).
[26]A. Ludviksson, K. H. Ernst, R. Zhang, and C. T. Campbell, J. Catal. **141**, 380 (1993).